

## Near-field optical patterning on azo-hybrid sol-gel films

N. Landraud, J. Peretti, F. Chaput, G. Lampel, J.-P. Boilot,<sup>a)</sup> K. Lahlil, and V. I. Safarov<sup>b)</sup>  
*Laboratoire de Physique de la Matière Condensée, UMR 7643-CNRS, Ecole Polytechnique,  
91128 Palaiseau Cedex, France*

(Received 2 August 2001; accepted for publication 29 October 2001)

We report on the near-field optical patterning of photochromic sol-gel films with subwavelength resolution. The sample containing functionalized azobenzene species is locally illuminated in the visible absorption band of these photochromes through the aperture of a metallized tapered optical fiber. The surface topography imaged by *in situ* shear-force microscopy reveals that, due to repeated photoisomerization cycles of the azobenzene molecules, photoinduced matter migration occurs under the tip leading to the formation of a surface relief. The shape of this structure is characteristic of the electromagnetic field distribution and strongly depends on the tip-to-sample distance. In near-field illumination conditions, protrusions of lateral dimension as small as 60 nm ( $\approx \lambda/10$ ) are currently produced. When repeating this process, compact arrays of nanodots are optically inscribed.

© 2001 American Institute of Physics. [DOI: 10.1063/1.1428627]

Near-field optics have been developed to overcome the diffraction limit of conventional optical methods and achieve lateral resolution much smaller than the wavelength.<sup>1,2</sup> But the interpretation of the contrast origin in near-field optical microscopy images is not obvious and unquestionable demonstrations of high optical resolution are not current. However, beyond the imaging applications, one can benefit from the potential high optical resolution of near-field optics to perform optical patterning of surfaces. In the present letter, we show that hybrid sol-gel films containing azobenzene derivatives can be optically patterned with a resolution of a tenth of the wavelength ( $\approx 50$  nm) by using near-field optical techniques.

It is now well-known that azobenzene groups in a polymeric matrix give rise to matter migration when illuminated in their visible absorption band.<sup>3,4</sup> By projecting an interference pattern on an azo-polymer film, surface relief gratings have been optically inscribed with a fringe separation of about 1  $\mu\text{m}$ , a high modulation depth (of the order of the film thickness) and a high diffraction efficiency.<sup>5,6</sup> The grating is formed with *p*-polarized illumination, i.e., if the light polarization vector has a nonzero component along the intensity gradient. This dependence on the light polarization excludes a thermal origin of this effect. The phenomenological description of the process is the following. The stable state of the molecule is the trans-isomeric configuration. The absorption of a photon induces the transition to the cis-isomer. This state is metastable and the reverse transition to the trans-state takes place by thermal activation. Therefore, a molecule absorbing a photon undergoes a complete trans-cis-trans isomerisation cycle. This transition induces a motion of the molecule and a related deformation of the matrix to which the molecule is grafted. This motion takes place in the direction of the light polarization and stops when the photochrome is

in a dark fringe of the interference pattern. Several models are proposed to describe the phenomenon,<sup>7-9</sup> but the microscopic mechanism which relates the photoisomerisation of the azobenzene molecule to the matter migration is not yet fully understood.

The experiments reported here were performed on sol-gel samples prepared from functionalized alkoxy silane monomers bearing bulky carbazole moiety (Si-K) and electron-donor/electron-acceptor substituted azobenzene (Si-DR1). The synthesis of silane-modified monomers has already been presented elsewhere.<sup>10</sup> To obtain solid-state materials, the functionalized monomers are copolymerized with a cross linking agent, the tetraethoxysilane (TEOS). In a typical sol preparation, alkoxy silanes (2 Si-DR1 + 4 Si-K + 1 TEOS) are dissolved in tetrahydrofuran and hydrolyzed with acidic water ( $[\text{H}_2\text{O}]/[\text{Si}] = 4$ ). The mixture is stirred for several hours, then pyridine is added to neutralize the acidity of the medium and enhance therefore the condensation reaction rate. Afterwards, the so-prepared hybrid sol is deposited by spin coating on a glass substrate, leading to a hybrid film of thickness that can be varied from 20 to 800 nm by adjusting the sol concentration and the angular velocity of the spin coater. Samples are not heat treated in order to keep a low condensation degree (weakly cross linked silica network). In Fig. 1, the organically modified silica network is schematized and the absorption spectrum of a Si-DR1/Si-K/TEOS hybrid film of thickness 75 nm is plotted. The broad band in the wavelength range between 400 nm and 600 nm is due to the azobenzene moieties.

The experimental set-up is a homemade aperture scanning near-field optical microscope schematized in Fig. 2. The tapered probe is produced by combining laser-heated pulling and acid etching of a single-mode fiber with core and cladding diameters of 3.7  $\mu\text{m}$  and 125  $\mu\text{m}$ , respectively. The fiber pulling is carried out with a homemade apparatus which allows one to produce a conical tip, with a cone angle of about 50° and a flat aperture of diameter varying from 400 to 1000 nm. The second step consists of a short chemical etching of the preformed tip with 13.4 wt % aqueous hydrofluoric

<sup>a)</sup> Author to whom all correspondence should be addressed; electronic mail: jean-pierre.boilot@polytechnique.fr

<sup>b)</sup> Permanent address: Groupe de Physique de l'Etat Condensé, UMR-CNRS 6631, Case 901, Département de Physique, Faculté des Sciences de Luminy, Université de la Méditerranée, 13288 Marseille Cedex.

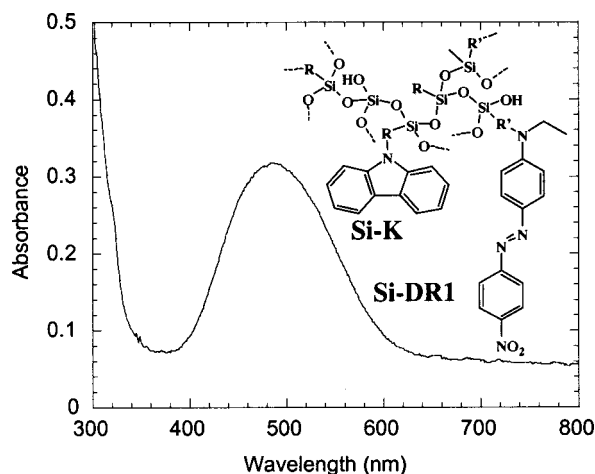


FIG. 1. Absorption spectrum of an azo-polymer film of thickness 75 nm.

acid. We made sure that the chemical etching is isotropic and preserves the taper angle while the diameter of the flat aperture is reduced. Finally, the etched tapered fiber is coated with a 10 nm-thick chromium layer and a 100 nm-thick aluminum layer, by evaporation in a secondary vacuum chamber. This allows to confine the light and to create a definite aperture at the tip apex with a typical diameter of about 50 nm.

The tip-to-sample distance is regulated by the shear-force technique.<sup>11</sup> The tapered optical fiber is attached to a dither piezoelectric tube which is excited at one of the resonance frequency of the free vibrating part of the fiber. The changes in the vibration amplitude of the tip due to the shear-force interaction with the sample surface are detected by measuring the variation of the electrical impedance of the dither piezo through a Wheatstone bridge and a lock-in amplifier.<sup>12,13</sup> We feedback control the tip-to-sample separation using a signal derived from this impedance change.

The yellow line of a Kr<sup>+</sup> laser, of wavelength  $\lambda = 568$  nm, is used as a light source. The power injected into the fiber is estimated at about 100  $\mu$ W. For an aperture diameter of 100 nm, the power emitted (in far field) by the tip is usually of 1 nW, leading to a power density of the order of 10 W cm<sup>-2</sup>. In a typical experiment, the tip is brought to a few nanometers to the film surface. The sample is then locally irradiated for a time of the order of a few seconds

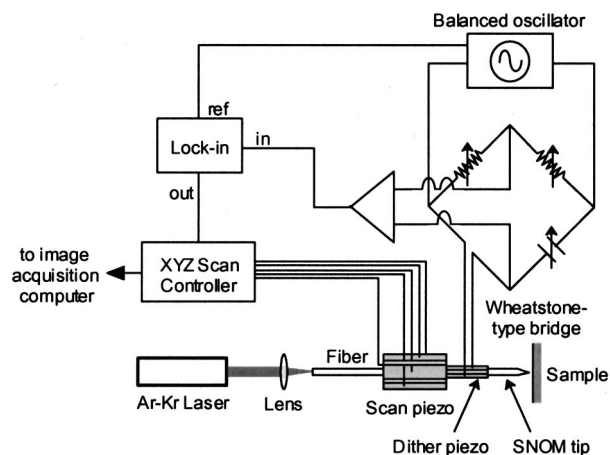


FIG. 2. Schematic view of the experimental setup.

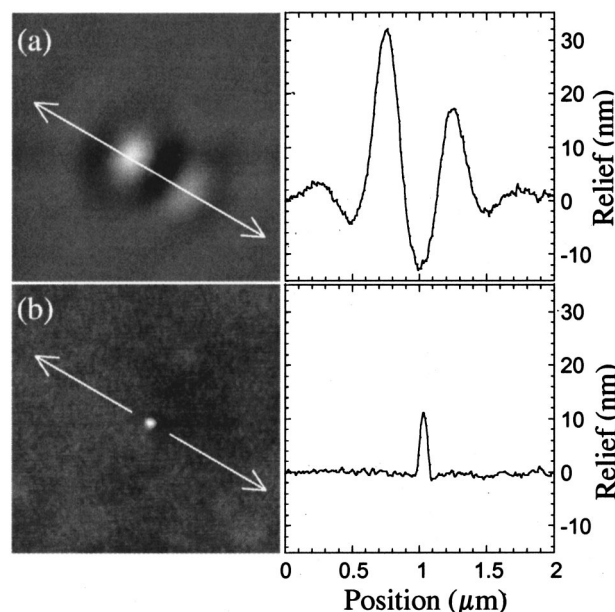


FIG. 3. (a) 2  $\mu$ m  $\times$  2  $\mu$ m shear-force image of the pattern inscribed on the photochromic film with a far-field illumination by the tip set at a distance to the sample of 130 nm. The light injected in the fiber is linearly polarized. (b) 2  $\mu$ m  $\times$  2  $\mu$ m shear-force image of the area where a local near-field illumination of the sample has been produced with a tip-to-sample distance smaller than 10 nm.

controlled by a mechanical laser beam shutter. The surface topography, modified according to the field map around the tip, is then read out *in situ* by recording the shear-force image of the processed area.

Figure 3(a) shows the 2  $\mu$ m  $\times$  2  $\mu$ m image of the surface after illumination when the tip was set at a distance to the sample of about 130 nm and the light injected in the fiber was linearly polarized. The irradiation has produced a 300 nm diameter hollow surrounded by two diametrical protrusions. In fact, this experiment corresponds to a far-field configuration since the tip-to-sample distance is larger than  $\lambda/2\pi$  ( $\approx 90$  nm).<sup>14</sup> Therefore, the azobenzene moiety behavior is similar to the one observed in the far-field experiments of surface relief grating printing just discussed. The azobenzene molecules tend to move (pulling the matter) away from the illuminated area, which leaves the hollow. This migration takes place along the direction defined by the light polarization and results in the formation of the two diametrical protrusions on both sides of the hollow. We have checked that, when the injected light polarization is rotated, the whole pattern (the hollow surrounded by the two diametrical protrusions) is rotated by the same angle.

Thereafter, if the tip is brought in the near-field of the film surface, typically at a distance smaller than 10 nm, the illumination produces a 65 nm-diameter circular protrusion [Fig. 3(b)]. Inversely to the far-field configuration, photoinduced matter migration leads here to a film swelling in the area irradiated by the tip. It is still generated by the azobenzene moiety movements subsequent to repeated trans-cis-trans isomerization cycles but according to an electric field distribution which is of course very different from the far-field one. These experiments give information about the field map around the emitting tip. Further investigations are in

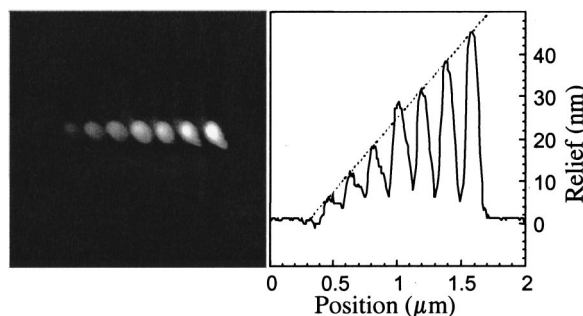


FIG. 4.  $2\ \mu\text{m}\times 2\ \mu\text{m}$  image of a line of seven protrusions inscribed in near-field with illumination times increasing linearly: 5, 10, 15, 20, 25, 30, and 35 s. The distance between two adjacent bumps is constant and equal to 180 nm.

progress to relate the optical near-field distribution to the induced relief pattern.

We have varied the irradiation dose by increasing the illumination time while keeping constant the light input power (Fig. 4). Circular protrusions are still formed in near-field (the apparent ovoid shape of the bumps is here only an artifact of the shear-force image due to the shape of the tip). As shown by the line plot across the protrusions, their diameter is constant and defined by the tip aperture (of about 120 nm in this experiment) and their height is directly proportional to the irradiation time. This definitely confirms that the protuberance formation is of pure near-field optical origin and that no thermal heating or threshold effects occur. We have performed the same experiment with a five times larger input power and divided the whole irradiation time by the same factor. This yields a similar pattern which is not reproduced here.

Figure 5 shows an example of a near-field surface patterning of a 20 nm-thick film with a  $\lambda/10$  resolution. An array made of  $9\times 9$  nanodots of 55 nm-lateral size (full width at half height) is inscribed in an area of  $1\times 1\ \mu\text{m}^2$ . The shear-force image is taken with a scanning direction rotated by  $45^\circ$  to avoid reading artifacts and the observed

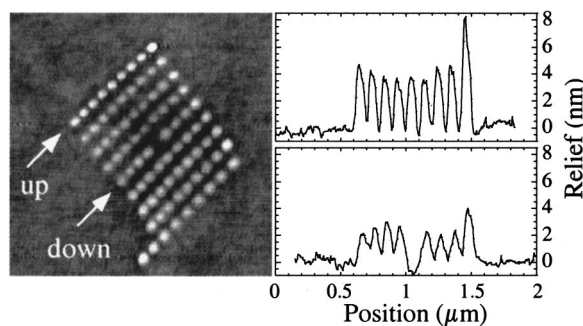


FIG. 5.  $2\ \mu\text{m}\times 2\ \mu\text{m}$  image of an array of  $9\times 9$  bumps inscribed in near-field on a 20 nm-thick film. The lateral size of each bump is 55 nm (full width at half height), the mean height of the bumps is 5 nm.

deformation of the “square” array is only due to piezoelectric nonlinearity. The profiles of two dot lines are also reported in Fig. 5. It is shown that each nanodot is well separated from its closest neighbors. Furthermore, the writing process is nondestructive as one dot is not erased when the next ones are inscribed. We have deliberately omitted the central dot, to show that the writing process is perfectly controlled. Note that such an experiment corresponds to a density of binary recorded data as high as  $80\ \text{bit}\ \mu\text{m}^{-2}$ .

To conclude, we have demonstrated the possibility to pattern thin photochromic sol-gel films with a nanometric resolution by using aperture near-field optical techniques. The formation of topographic structures of subwavelength size is due to the matter migration induced by repeated photoisomerization cycles of the azobenzene derivatives grafted in the sol-gel matrix. The results reveal the difference in the field distribution whether the illuminating tip was brought in right proximity of the film surface (near field) or at about a hundred nanometers away (far field). With near-field illumination, the lateral size of the structures is defined by the tip aperture diameter. The height of the protrusion is directly proportional to the irradiation dose. As the illumination is strictly confined under the tip, compact arrays of bumps with nanometric lateral size can be inscribed without neighbor erasing effects. This demonstrates a near-field optical resolution of  $\lambda/10$  and provides potential applications to optical nanolithography and high density optical data storage with a capacity of at least  $1\ \text{Gbyte}\cdot\text{cm}^{-2}$ . Our photoresponsive material also exhibits capabilities to map the electromagnetic field distribution in the vicinity of a nanometric object. This property can be of great help to improve comprehension of near-field optical measurements.

<sup>1</sup>E. Betzig, J. K. Trautman, T. D. Harris, J. S. Weiner, and R. L. Kostelak, *Science* **251**, 1468 (1991).

<sup>2</sup>B. Hecht, B. Sick, U. P. Wild, V. Deckert, R. Zenobi, O. J. F. Martin, and D. W. Pohl, *J. Chem. Phys.* **112**, 7761 (2000).

<sup>3</sup>P. Rochon, E. Batalla, and A. Natansohn, *Appl. Phys. Lett.* **66**, 136 (1994); D. Y. Kim, S. K. Tripathy, L. Li, and J. Kumar, *Appl. Phys. Lett.* **66**, 1166 (1994).

<sup>4</sup>S. Davy and M. Spajer, *Appl. Phys. Lett.* **69**, 3306 (1996).

<sup>5</sup>X. L. Liang, L. Li, J. Kumar, D. Y. Kim, V. Shivshankar, and S. K. Tripathy, *Appl. Phys. Lett.* **68**, 2618 (1996).

<sup>6</sup>B. Darracq, F. Chaput, K. Lahlil, Y. Levy, and J.-P. Boilot, *Adv. Mater.* **10**, 1133 (1998).

<sup>7</sup>C. J. Barrett, P. L. Rochon, and A. L. Natansohn, *J. Chem. Phys.* **109**, 1505 (1998).

<sup>8</sup>P. Lefin, C. Fiorini, and J.-M. Nunzi, *Pure Appl. Opt.* **7**, 71 (1998).

<sup>9</sup>K. Sumaru, T. Yamanaka, T. Fukuda, and H. Matsuda, *Appl. Phys. Lett.* **75**, 1878 (1998).

<sup>10</sup>F. Chaput, D. Riehl, J.-P. Boilot, T. Gacoin, M. Canva, Y. Levy, and A. Brun, *Mater. Res. Soc. Symp. Proc.* **435**, 583 (1996); F. Chaput, K. Lahlil, J. Biteau, J.-P. Boilot, B. Darracq, Y. Levy, J. Peretti, V. I. Safarov, A. Fernandez-Acebes, and J.-M. Lehn, *Proc. SPIE* **3943**, 32 (2000).

<sup>11</sup>E. Betzig, P. L. Finn, and J. S. Weiner, *Appl. Phys. Lett.* **60**, 2485 (1992).

<sup>12</sup>J. W. P. Hsu, M. Lee, and B. S. Deaver, *Rev. Sci. Instrum.* **66**, 3177 (1995).

<sup>13</sup>P. Bertrand, L. Conin, C. Hermann, G. Lampel, J. Peretti, and V. I. Safarov, *J. Appl. Phys.* **83**, 6834 (1998).

<sup>14</sup>D. Courjon and C. Bainier, *Rep. Prog. Phys.* **57**, 989 (1994).